RNA-Seq And WGCNA Analysis Identifies Salt-Responsive Genes In Pear (*Pyrus Ussuriensis* Maxim)

Qiming Chen
Nanjing Agricultural University
Huizhen Dong
Nanjing Agricultural University
Zhihua Xie
Nanjing Agricultural University
Kaijie Qi
Nanjing Agricultural University
Xiaosan Huang
Nanjing Agricultural University
Shaoling Zhang (slzhang@njau.edu.cn)
Nanjing Agricultural University

Research Article

Keywords: Pyrus, Dynamic transcriptome, High salt stress, WGCNA, Plant signal transduction

Posted Date: September 23rd, 2021

DOI: https://doi.org/10.21203/rs.3.rs-847089/v1

Abstract

Background: Pear is one of the most abundant fruit crops and has been cultivated world-wide. However, the salt injury events caused by increased salinity limited the distribution and sustainable production of pear crops. Therefore, it is needed to take further efforts to understand the genetics and mechanisms of salt tolerance to improved salt resistance and productivity.

Results: In this work, we analyzed the dynamic transcriptome of pear (*Pyrus ussuriensis* Maxim) under salt stress by using RNA-Seq and WGCNA. A total of 3540, 3831, 8374, 6267 and 5381 genes were identified that were differentially expressed after exposure to 200mM NaCl for 4, 6, 12, 24 and 48 hours, respectively, and 1163 genes were shared among the five comparisons. KEGG enrichment analysis of these DEGs (differentially expressed genes) revealed that “MAPK signaling” and “Plant hormone signal transduction” pathways were highly enriched. Meanwhile, 622 DEGs identified from WGCNA were highly correlated with these pathways, and some of them were able to indicate the salt tolerance of pear varieties. In addition, we provide a network to demonstrate the time-sequence of these co-expressed MAPK and hormone related genes.

Conclusion: A comprehensive analysis about salt-responsive pear transcriptome were performed by using RNA-Seq and WGCNA. We demonstrated that “MAPK signaling” and “Plant hormone signal transduction” pathways were highly recruited during salt stress, and provided new insights into the metabolism of plant hormones related signaling at transcriptome level underlying salt resistance in pear. The dynamic transcriptome data obtained from this study and these salt-sensitive DEGs may provide potential genes as suitable targets for further biotechnological manipulation to improve pear salt tolerance.

Background

Abiotic stresses, such as high salinity, drought and low temperature, are the major factors that affect plant growth and development. Among them, high salinity is the main environmental factor that hinders plant growth and restricts crop yield [1,2]. Plants have evolved a series of different adaptive mechanisms in order to resist high salt stress, one of which is to obtain salt tolerance after experiencing salt stress [3]. However, plant salt tolerance which controlled by multiple gene regulatory network, is a complex process affected by many signaling transduction pathways, including signaling transducers, transcription factors and stress responsive genes and metabolites [4].

A great effort has been made to understand the mechanism of plant salt tolerance, which is mainly focused on *Arabidopsis thaliana* [5]. Several important pathways of salt stress signal transduction have been identified, although there are still some uncertainties. Mitogen-activated protein kinase (MAPK) pathway which play important role in the response to salinity, as well in the signaling of plant hormones and the cell division, as well the salt overly sensitive (SOS) pathway and the Calcium Dependent Protein Kinase (CDPK) pathway play important roles in osmotic stress [6-9]. In recent years, a large number of studies have been carried out on the molecular basis of plant salt tolerance, and many genes related to

salt tolerance have been identified and characterized, including common transcription factors (TFs) AP2/ERF, bZIP, C2H2, WRKY, MYB, NAC and a huge number of stress responsive DREB families [10,11]. By binding to *cis*-acting elements in promoter region of genes, TFs systematically control gene expression in almost all processes of growth, development and against bio-/abiotic stresses. Meanwhile, plant hormones also have vital roles in those process and recruited parallel downstream pathways with MAPK signaling. Abscisic acid (ABA), auxins, cytokinins (CK), giberellic acid (GA) and ethylene were all well-known intracellular second messenger molecules and have been reported to play essential roles during high-salinity exposure [12]. The role of ABA that modulating various genes in response to water deficiency and salt stress is very important. There have been reported that, when plants undergo salinity stress, the auxin pathway were recruited, and the overexpression of *YUCCA3*, an auxin biosynthetic related gene, caused higher auxin concentration and hypersensitivity to salt stress. Ethylene was also generally regarded as stress-related hormone with a biological link to salinity signaling. Among the different plant hormones involving in responding to salt stress, GA has been especially important in crops such as wheat and rice. However, in response to salt stress, the function of every single plant hormone was not independent. Numerous reports have shown that different pathways are interconnected and coordinately regulate the plant response to biotic and abiotic stresses [13,14].

To date, based on the rapid development of high-throughput techniques，a number of plant genome-wide expression profiling under salt stress have been identified and characterized in many species, including rice, tomato, barley, sweet potato and maize [14]. But there is still little information available about the network dynamics involved in pear salt resistance. Pear is one of the most abundant fruit crops and has been cultivated world-wide. However, the salt injury events caused by increased salinity limited the distribution and sustainable production of pear crops. Therefore, further efforts to understand the genetics and mechanisms of salt tolerance with the aim to improved salt resistance and productivity were needed [15]. With the releasing of the genome sequence of pear [16], RNA sequencing (RNA-Seq) data, which mapped to a high-quality reference genome, could provide more reliable evidences to understand the underlying mechanism of the salt resistance in pear [17].

In this study, we performed differentially gene expression analysis based on RNA-Seq analysis and WGCNA (weighted gene co-expression network analysis) to explore the inner link between the gene expression pattern and the salt resistance of pear. In addition, we provided some new insights into the metabolism of plant hormones related signaling at transcriptome level underlying salt resistance in pear, and opened up the possibility of salt resistance breeding by manipulating specific genes in plant hormones pathways.

Results

Analysis of biochemical indicators after salt treatment and preparation of transcriptome samples

We performed salt treatment on pear tissue culture seedlings with 200 mM NaCl (Fig. 1A). However, during the first 24 hours of salt stress, the phenotype of seedlings was not visibly changed,

and the leaf edges and tender shoots began to brown at 48 h after treatment (Fig. 1A). In order to explore the effect of salt stress on pears, the components which reflecting the degree of cellular damage were measured, including the malondialdehyde (MDA) content, proline (Pro) content and reactive oxygen species (ROS) level. Although, no significant phenotypic change was observed until 24 hpt (hour post treatment), all these biochemical indicators have changed significantly. After 6-hour salt treatment, the peak MDA content was detected during an upward tendency, and then dropped to its lowest value till 24 hpt (Fig. 1B). From 4 hpt to 12 hpt, the content of proline was continuously declined to the lowest value followed by a sharp rise to the peak (Fig. 1C). Previous studies have been shown that, by exposure to high salinity and low temperature, the plants recruit oxidative burst as the first response [18] and the level of ROS is able to reflect the cellular components damage degree [19,20]. O_2^- and H_2O_2 are two major forms of ROS in plant aerobic metabolism [21]. The measurement of ROS level showed that, like the rising trend of MDA, exposure to salt stress for 4 h caused remarkable rise of H_2O_2, which maintained stable until 6 h (Fig. 1D). However, high intracellular ROS content could also cause damage, therefore, H_2O_2 was decreased at 12 hpt along with the peak level of anti-O_2^- activity (Fig. 1E). The results were consistent with the works of Huang and Jin [22,23] that, salt treatment resulted in cell damage and higher ROS content, indicating that the stress treatment system in this study is reliable [24].

RNA-Seq of *Pyrus ussuriensi* under salt stress

The quality of the cDNA libraries from 18 samples (three biological replicates were collected for each of six time points) was shown in Table 1. The number of raw reads and mapping rate for these libraries ranged from 43 to 53 million and 72.37–75.77%, respectively, with an average Q20 (sequencing base calls with an error rate of<1%) of >95%. The data quality was high enough for further analysis. The density distribution profiles of fragments per kilobase transcript per million mapped reads (FPKM) were constructed to display the gene expression pattern of each sample (Fig. 2A). Principal component analysis (PCA) was performed to reveal the differences in the expression of genes during the six treatment time points, based on the Pearson correlation of FPKM values (Fig. 2B). As the result shown in Fig. 2B, six distinct sample groups were identified. The differences between each group were obvious, while the differences within the groups were small, which indicated that the transcription program of different treatment time had changed significantly.

Comparison of transcriptional profiles of genes involved in salt stress response

In order to investigate the relationship between gene expression and phenotype changes, differences in gene expression during salt treatment were analyzed. We believed that DEGs related to salt treatment mainly exist between S0 and S4, S0 and S6, S0 and S12, S0 and S24, S0 and S48, which resulted in five pairs of comparisons. As shown in Fig. 2C, 3540, 3831, 8374, 6267 and 5381 DEGs were detected from five comparison groups (S0 vs S4, S0 vs S6, S0 vs S12, S0 vs S24 and S0 vs S48), respectively, and 1163 DEGs were shared. In addition, there 559□267□2207□494 and 610 DEGs were uniquely in each group. Then, gene ontology (GO) and Kyoto Encyclopedia of Genes and Genomes (KEGG) pathway enrichment analyses were performed to improve our understanding of the functions of 1163 DEGs (Fig. S1). The

significantly enriched gene pathways involving DEGs following the salt stress treatment were showed in Table 2.

GO enrichment analysis annotated about 35 terms, which were subsequently categorized into 20 GO functional group. In these groups, the thylakoid part has the highest enrichment degree, and the chloroplast part and plastid part have the largest number of enrichments (Fig. S1A). Previous reports have described the complex biological processes involved in salt stress including stress recognizing sensor proteins, signaling transducers, metabolites, transcription factors and stress responsive genes. Therefore, the KEGG enrichment analysis of these 1163 DEGs were performed (Fig. S1B). According to the enrichment results, two highly enriched pathways, MAPK signaling and plant hormone signal transduction pathways, were selected for subsequent analyses (Fig. S1B). The present results were consistent with the overall biochemical pathways that are known to be activated during salt stress [14].

To reveal the expression pattern of these enriched genes, we built a heat map of plant hormone signal transduction and MAPK signal pathways (Fig. 2D). In total, 34 DEGs were enriched in these two pathways, including 15 genes from hormone pathway, six from MAPK pathway and 13 involved in both two pathways, such as *ERF1s* and *PP2Cs* (Fig. 2D). As shown in Fig. 2D, most enriched DEGs were up-induced by salt treatment and the expression peaks of them mostly occurred at from S4 to S24. The other down-induced DEGs displayed a sustained downward trend. It is notable that the expression levels of an auxin related downstream gene *SAUR* (*Pbr039046.1*) was extremely high since the up-regulating from S4 stage (Fig. 2D and Fig. S3).

Identification of gene co-expression modules related to high salinity treatment

In order to perform WGCNA analysis, 14743 detected DEGs (at least in one of five comparison groups) were selected and 11057 genes remained (automatically filtered by WGCNA package). Then, we determined the soft-thresholding powers of the network. As shown in Fig. 3, power 24 was selected to build a hierarchical cluster tree (Fig. 3A), and remained genes were grouped into 12 distinct modules (labeled with different colors), according to the major tree branches (Fig. 3B). The largest module contained 2025 genes, whereas the smallest module contained only 66 genes. Furthermore, we associated each co-expression module with stages of salt stress and the content of H_2O_2, O_2^-, Pro and MDA of each stage (Fig. 3C), in which four co-expression modules showed a relatively higher correlation ($r \geq 0.60$ and $p < 0.01$) with these biochemical indicators. However, only the module “black” was highly correlated with salt treatment (r=0.86, p=5x10^{-6}) and the content of H_2O_2 (r=0.68, p=0.002) and Pro (r=0.79, p=9x10^{-5}) (Fig. 3C). Therefore, we focused on the genes in black module. The expression heat map of module black showed two main different gene clusters, and the expression peaks under salt treatment of each cluster were various in the early (from S0 to S12) or late stages (S24 and S48) (Fig. 4A). Meanwhile, 49 TF-encoding genes from 14 families were identified in the black module (Fig. 4B). Among them, the largest family of transcription factors was the AP2/ERF family. A total of eight AP2/ERF genes were identified as salt-responsive TF in this study. In addition, other bio-/abiotic stress responding TF families were also detected, including HB family, bZIP family, C2C2 family and TCP family with

relative high gene numbers which were consistent with the salt stress phenotype, demonstrating the accuracy of the screening module. Further enrichment analysis of genes in module black (Fig. 4C) showed that 12 genes and 14 genes, which were the most two of all displayed pathways, were enriched in MAPK signaling and plant hormones signal transduction pathways, respectively, indicating that these genes are most likely involved in the process responding to salt stress and MAPK signaling and plant hormones signal transduction pathways might play vital roles for plants to resist against salt stress.

To further understand the involvement of MAPK signaling and hormones signal transduction in salt stress response, we combined the genes enriched in these two pathways from module black and the shared 1163 DEGs, and finally obtained 49 genes (40 related to hormones, 30 related to MAPK pathway and 21 genes were overlapped) (Fig. 4C and Fig. S2). Then we constructed the protein-protein interaction network with the correlations data among these 49 DEGs, and we replaced them based on the relationship to different plant hormones (the hormone-related DEGs were displayed in Table 3) and signaling pathways (Fig. 4D). With the different expression patterns of each gene cluster, the time-sequence of these co-expressed genes can be clearly demonstrated. For example, after four hours salt stress treatment, genes related to Ca^{2+} and ethylene were initially upregulated, accompanied by the upregulating of most of ABA and auxin related genes (most of *PP2Cs* and *ABF* from ABA signaling, some of *IAAs* and *SAUR* from auxin pathway). Meanwhile, *PYLs* from ABA signaling and *AUX1*, *GH3* and some of other *IAAs* and *SAURs* were significantly down-regulated. During the treatment time from six hours to 24 hours, the expression peaks of each gene clusters were showed up. As the pathway with the earliest expression peak, the peak for ethylene signaling related genes uniformly appeared at S6 stage, followed by the peak of *RBOH*, *MPK3* and a *CALM* (*Pbr039046.1*) from Ca^{2+} related genes and TF *WRKY33s* at S12 stage. Subsequently, the relative late expression peaks appeared at S24 stage on *PP2Cs*, *ABF* and *SNRK* from ABA signaling, another two *CALMs* and some of *IAAs* and *SAURs* from auxin pathway. Significantly, at different time points of salt treatment, the main hormone-related genes recruited by plants were different at transcriptional level.

To validate the RNA-Seq data, 12 DEGs were randomly selected to perform real-time quantitative reverse transcription-polymerase chain reaction (qRT-PCR) analysis. As shown in Fig. S3, the relative expression level of these DEGs obtained by qRT-PCR were highly consistent with RNA-Seq data for most of the tested genes. This result supports the reliability of the RNA-Seq analysis.

Evidence of the connection of predicted genes and salt tolerance

High salt stress can cause local necrosis of a plant leaf, and the dark/green ratio of treated leaf is negatively correlated with salt tolerance. To verify the connection between genes and salt tolerance, the dark/green ratio of mature leaves of different pear cultivars were determined (Fig. 5A and B). Under the treatment, wild pear ‘Duli’ showed a relative high tolerance to salt stress with the lowest final leaf darken ratio followed by cultivars ‘Dangshan’ and ‘Xinli NO.7’ with medium tolerance. The final darked ratios of salt-sensitive pear ‘Huangguan’ and ‘Xueqing’ reached 87.8% and 95.7%, respectively. Meanwhile, we

obtained the transcript profiles of six verified sensitive-to-salt DEGs at 0, 4, 6, 12, 24 and 48 hpt of these cultivars, and all of them were differentially expressed under salt stress to varying degrees (Fig. 5C). Linear regression analysis between gene expression and dark/green ratio, shown in Fig. 5D, revealed that the expression of *IAA* (*Pbr025864.2*) was positively correlated with the ratio changes of high and medium salt tolerant varieties 'Duli', 'Dangshan' and 'Xinli NO.7' and negatively correlated with that of other two salt-sensitive cultivars. In addition, the transcript levels of the genes encoding *ERF* (*Pbr030542.1*), *PP2C* (*Pbr009416.1*) and *SAUR* (*Pbr041090.1*) have a strong negative correlation with the dark/green ratio of salt-sensitive cultivars, while *WRKY33* (*Pbr034115.1*) is positive correlated with that in 'Xinli NO.7'. This analysis of different cultivars provides correlative evidence that these DEGs were directly or indirectly involved in the regulation of the tolerance of pear to salt stress, and might be considered as indicators of the salt tolerance of pears after the further functional characterization (Fig. 5).

Discussion

In this study, we firstly performed salt treatment on tissue culture seedlings of 'Qiuzi' pear (*Pyrus ussuriensis* Maxim) to measure the effect of salt treatment on pear. Although, the visible darken on leaves was observed until 48 hpt of salt treatment, the content of biochemical indicators had showed significant variation from 4 hpt, indicating that biochemical and transcriptional changes were prior to the physiological changes. Then, the dynamic transcript profiles of pear seedlings under NaCl treatment were investigated by RNA-Seq. For each time point, three samples were used as biological replications. There were from 43 to 53 million clean reads for each library for each sample, with all Q20 >96% and a mapping rate of 72.37–75.77%, indicating sequencing quality of these data were high enough downstream analysis (Table 1). Furthermore, the PCA analysis revealed six relative distinct sample groups and the other five groups were far away from the control group, suggesting that significant transcriptional changes occur across these time points with salt stress (Fig. 2B). Therefore, we believed that DEGs related to salt treatment mainly exist between samples of each treating time point to untreated samples.

Comparative analysis revealed that 3540, 3831, 8374, 6267 and 5381 DEGs were detected in the five group pairs, respectively (Fig. 2C). The DEG number peak were detected at S12 stage, which means that there were significant changes in transcriptional levels between S0 and S12. KEGG enrichment analysis showed that, except for the living-necessary processes (such as carbon sequestration Photosynthesis, Ribosome and Carbon fixation), Glutathione metabolism pathway was only highly enriched in S12 stage with 55 DEGs (Table 2). Glutathione was an important compound that regulates *in vivo* re/dox balance and responds to multiple bio-/abiotic stresses. The large number of enriched DEGs from Glutathione metabolism pathway suggested that this pathway might play an important role in the salt tolerance response of plants at this stage. As for other four stages, plant hormone signal transduction pathway was all highly enriched with the largest number of each, followed by MAPK signaling pathway, indicating that genes related to plant hormones and MAPK signaling might also make crucial contribution to salt

tolerance of plants throughout the entire response processes (Table 2). In addition, these five comparison groups shared 1163 DEGs, and the enrichment analysis likewise highlighted 34 DEGs enriched in these two pathways with top two gene numbers (Fig. 2D), which was consistent with the forementioned results. Furthermore, the FPKM value heatmap revealed that the most of these 34 DEGs were up-regulated from S4 stage and the peak expression showed up at S6 or S12 stage, which means Plant hormone signal and MAPK signaling pathways were continuously recruited at all stages in response to salt stress.

WGCNA was further performed to identify the candidate salt resistance-linked genes. We identified 11 distinct modules with gene numbers arrange from 66 to 2025 of each (Fig. 3A and B). Although, three co-expression modules were highly correlated with the salt treatment, only module MEblack was selected as candidate module for the highest correlation (Fig. 3C). Expression heatmap constructed of 622 DEGs from module black clearly displayed two different expression patterns with diverse directions of regulation and various treating time of the detected expression peak (Fig. 4A). TFs play critical roles in regulating salt resistance in plants, and several important TFs involved in abiotic stress responses have been identified, inclusing AP2/ERF, bZIP, C2C2 and WRKY. Meanwhile, we identified 49 TF-encoding genes from 14 families including many bio-/abiotic stress responding TF families, such as AP2/ERF family, HB family, bZIP family, C2C2 family and TCP family which were with relative high gene numbers (Fig. 4B). We believed that these identified stress-related TF-DEGs were deeply involved in the salt resistance responses, and able to provide candidate genes for subsequent salt tolerance breeding in pear.

The KEGG pathway enrichment result was also consistent with previous results that Plant hormone signal and MAPK signaling pathways were highly recruited during the salt stress treatment. The two pathways deeply and intricately overlapped with each other. Consequently, to further investigate the involvement of MAPK signaling and plant hormone signal transduction during the salt stress, we built a network by using 49 combined DEGs from these two pathways (Fig. 4D). Together with the separated heatmaps for each signaling process, the composite network based on the relationship to different hormones and signaling pathways was able to clearly demonstrate the time-sequence of these co-expressed genes (Table 3 and Fig. 4D). As shown in Fig. 4D, ethylene related pathway was initially activated at very early stage and the expression peaked at 6 hours after salt stress with the first peak of ABA pathway. Then, parts of Ca^{2+} and auxin related genes were significantly induced to high expression levels from S6 to S12. At later stages of salt stress, ABA signaling process was reactivated to a secondary peak at S24 stage, as well two Ca^{2+} related *CALM* genes were up-regulated to the peak. It was notable that the expression patterns of *PP2Cs*, *WRKY33s* and all ethylene related genes from each pathway were highly consistent, which meant these similar-pattern genes might be functionally conservative and regulated by relatively conserved upstream transcriptional regulation. In addition, by investigating the connection between gene expression and salt tolerance of different pear varieties, we obtained several sensitive-to-salt DEGs which might be considered as indicators of the salt tolerance of pears.

In summary, the comprehensive data presented here will serve as a robust resource for understanding salt resistance responses of pear, particularly the broad and continuous recruiting of MAPK signaling and

plant hormone signal transduction pathways in pear under salt stress. To date, our understanding of how pear resist salt stress remains limited. Future studies will focus on the candidate MAPK signaling and hormones related genes involved in the response to high salinity. And the upstream transcriptional regulators of them also needed to be identified and further investigated.

Conclusion

In this work, we analyzed the dynamic transcriptome of pear (*Pyrus ussuriensis* Maxim) under salt stress by using RNA-Seq and WGCNA. A total of 3540, 3831, 8374, 6267 and 5381 genes were differentially expressed under 200mM NaCl for 4, 6, 12, 24 and 48 hours, respectively. Functional enrichment analyses revealed that “MAPK signaling” and “Plant hormone signal transduction” pathways were highly recruited during salt stress. Meanwhile, WGCNA of DEGs identified 622 genes which were highly correlated with these pathways, and some of them were able to indicate the salt tolerance of pear varieties. In addition, we provided some new insights into the metabolism of plant hormones related signaling at transcriptome level underlying salt resistance in pear, and opened up the possibility of salt resistance breeding by manipulating specific genes in plant hormones pathways. The dynamic transcriptome data obtained from this study and these salt-sensitive DEGs may provide potential genes as suitable targets for further biotechnological manipulation to improve pear salt tolerance.

Methods

Plant materials and salt treatment

The tissue culture seedlings of ‘Qiuzi’ pear (*Pyrus ussuriensis* Maxim) were grown in the greenhouse under 16 h light/8 h dark, 75% relative humidity and at 26°C. Healthy and same growth state plants were inserted into a beaker containing distilled water for 2 d before the salt treatment. Then seedlings were put into 200 mM NaCl for salinity stress treatment and allowed to salt stress for 0, 4, 6, 12, 24 and 48 h.

For the salt treatment of field-grown mature plants, five pear varieties with different salt tolerance, ‘Duli’ (DL), ‘Dangshansuli’ (DS), ‘Huangguan’ (HG), ‘Xinli NO.7’ (XL7) and ‘Xueqing’ (XQ), were selected which were cultivated in Jiangpu farm in Nanjing Agricultural University. Five 50-centimeter-long branches of each variety from 2 or 3 trees were cut off and the bases of each branch were immersed in distilled water overnight at the same greenhouse condition. Then, the branches were transferred into 200 mM NaCl to perform treatment for 0, 4, 6, 12, 24 and 48 h. The dark/green ratio of treated leaves was measured by comparing the pixel value of the black area to the that of whole leaf by ImageJ software. At each treatment time point, the leaves were harvested independently, then placed in liquid nitrogen and stored at −80°C immediately.

RNA extraction and RNA-Seq library construction and sequencing

Total RNA extraction was performed by using Plant RNA Isolation Kit (Auto Lab) followed by the RNA purification using the RNeasy MiniElute Cleanup Kit (TIANGEN), according to the manufacturer's instructions. RNA purity and integrity was examined using the NanoPhotometer® spectrophotometer (IMPLEN, CA, USA) and the RNA 6000 Nano Assay Kit of the Bioanalyzer 2100 system (Agilent Technologies, CA, USA).

Library construction and RNA-seq were performed by Novogene company (Beijing, China). Briefly, high-quality total RNA (RIN ≥8) of three biological replicates of six samples (18 in total, one microgram RNA of each) was processed using a TrueSeq RNA Sample Prep kit (Illumina Technologies) for library construction. Sequencing libraries were generated using NEB Next Ultra RNA Library Prep Kit for Illumina (NEB). Library fragments were purified using the AMPure XP system (Beckman Coulter, Beverly, USA) to select cDNA fragments of preferentially 150–200 bp in length. And library quality was assessed on the Agilent Bioanalyzer 2100 system. Libraries were sequenced using Illumina HiSeqTM 2000.

Sequence data processing and mapping reads to the pear genome

Firstly, FASTQ format raw data (raw reads) were processed through inhouse Perl scripts. In this step, by removing reads containing an adapter or ploy-N and with low quality from the raw data, clean data (clean reads) were obtained and mapped to the pear genome data [16]. The reference genome index generation and paired-end alignment were performed by Hisat2 v2.0.4. Gene expression level was calculated using FPKM method, based on the length of a gene and the read counts mapped to it.

DEGs, functional annotation and pathway enrichment analysis

Differential gene expression analysis of samples was performed by R package: DESeq2 (v1.18.1) based on FPKM. In order to control the false discovery rate (FDR), the P-values were adjusted using [25] approach. Differentially expressed gene was assigned as the gene with an adjusted P-value of <0.001, absolute log2 fold change of ≥2 and with the FPKM of >1 in at least one sample.

GO was used to perform the function enrichment analysis of DEGs [26]. Significantly enriched GO terms were defined as the term which with a P-values of ≤0.05. The gene annotation was also analyzed using KOBAS (v2.0) (http:// kobas.cbi.pku.edu.cn/) to explore the statistical enrichment of DEGs in KEGG pathways. Significantly enriched KEGG pathways were defined as the pathway mapped by DEGs with the P-values of ≤0.05. The composite column graphs of enrichment analysis results and KEGG pathway graphs with expression levels were constructed by R package: ggplot2, respectively.

Gene co-expression network

R package: WGCNA was used to find clusters (modules) of highly correlated genes and to construct a co-expression network [27]. A minimum module size of 30 and a height cutoff of 0.26 were used to merge similar transcripts. We determined the correlation between each ME and the salt treating time as described previously [28], to determine the association of a module with stage-specific expression along

the treating time and the content of H_2O_2, O_2^-, Pro and MDA of each stage. Protein-protein interaction (PPI) analysis of the members in MEblack was performed based on the STRING database, and the PPI network were visualized using Cytoscape v.3.9.0.

TF analysis

TFs in MEblack were identified by aligning the protein sequences against the plant TF database PlntTFDB (v3.0, http://plntfdb.bio.uni-potsdam.de/v3.0/) [29]. Plant TFs were obtained and analyzed by using BLASTX with an e-value of $\leq 10^{-10}$. Finally, annotated TFs were classified into various groups according to the PlntTFDB v3.0.

QRT-PCR validation of DEGs

qRT-PCR were performed with 12 randomly selected DEGs. Specialized primers of selected genes were designed using the method described previously [30] (Supplementary Table S1). Pear tubulin (*Pbr042345.1*) was used as housekeeping gene with the LightCycler 480 SYBR Green Master (Roche, USA) system. The qRT-PCR assays were conducted with three technical copies. qRT-PCR reactions (20 μl per hole) were performed as previously reported [30]. The $2^{-\Delta\Delta Ct}$ method was used to evaluate the relative expression with Duncan's multiple range test.

Data analysis

Data processing was performed using R and Microsoft Excel. The box plot, principal component analysis plot, heatmaps and Venn diagram were all constructed by TBtools v1.089 [31].

Abbreviations

DEGs: differentially expressed genes; MAPK: mitogen-activated protein kinase; SOS: salt overly sensitive; CDPK: calcium dependent protein kinase; TF: transcription factor; ABA: abscisic acid; CK: cytokinins; GA: giberellic acid; RNA-Seq: RNA sequencing; WGCNA: weighted gene co-expression network analysis; MDA: malondialdehyde; Pro: proline; ROS: reactive oxygen species; hpt: hour post treatment; PCA: principal component analysis; FPKM: fragments per kilobase transcript per million mapped reads; GO: gene ontology; KEGG: Kyoto Encyclopedia of Genes and Genomes; DL: Duli; DS: Dangshansuli; HG: Huangguan; XL7: Xinli NO.7; XQ: Xueqing; FDR: false discovery rate; PPI: protein-protein interaction; CNGBdb: China National GeneBank DataBase; CNSA: CNGB Sequence Archive.

Declarations

Acknowledgements and Funding

This work has been supported by the National Key Research and Development Program of China (2018YFD1000303), the National Science Foundation of China (31872070; 32072538), the Jiangsu

Agriculture Science and Technology Innovation Fund (CX(18)3065), the Excellent Youth Natural Science Foundation of Jiangsu Province (SBK2017030026), the Project Funded by the Priority Academic Program Development of Jiangsu Higher Education Institutions, and the Earmarked Fund for China Agriculture Research System (CARS-28). Bioinformatic analysis was supported by the Bioinformatics Center of Nanjing Agricultural University.

Availability of data and materials

All data generated or analysed during this study are included in this published article and its supplementary information files. All needed sequence files and annotation files of Chinese white pear were obtained from the Nanjing Agricultural University pear genome project website (http://peargenome.njau.edu.cn) [16]. Plant TF database (PlntTFDB v3.0: http://plntfdb.bio.uni-potsdam.de/v3.0/) was used to identify the potential transcription factors [29]. The raw data that support the findings of this study have been deposited into CNGB Sequence Archive (CNSA: https://db.cngb.org/cnsa/) [32] of China National GeneBank DataBase (CNGBdb: https://db.cngb.org/) [33] with the project number CNP0002012.

Author's contributions

Q.C. and H.D. conceived and designed the experiments. Q.C. and X.H. carried out the experimental design. Q.C. analyzed data and drafted the manuscript. H.D. managed the tissue cultures of pear seedling and performed the experiment. Q.C. and Z.X. wrote the manuscript. K.Q. contributed experimental materials. Z.X. and S.Z. managed the research and experiments.

Ethics approval and consent to participate

Not applicable.

Consent for publication

Not applicable.

Competing interests

The authors declare that the research was conducted in the absence of any commercial or financial relationships that could be construed as a potential conflict of interest.

References

1. Zhu, J. K. Salt and drought stress signal transduction in plants. Annu. Rev. Plant Biol. 53, 247–273 (2002).

2. Huang, GT., Ma, SL., Bai, LP. et al. Signal transduction during cold, salt, and drought stresses in plants. Mol Biol Rep 39, 969–987 (2012).

3. Numan, M. et al. Plant growth promoting bacteria as an alternative strategy for salt tolerance in plants: A review. Microbiol. Res. 209, 21–32 (2018).

4. Ryu, H. & Cho, Y. G. Plant hormones in salt stress tolerance. J. Plant Biol. 58, 147–155 (2015).

5. Zhu, J. K. Plant salt tolerance. Trends Plant Sci. 6, 66–71 (2001).

6. Zhang, T. et al. Diverse signals converge at MAPK cascades in plant. Plant Physiol. Biochem. 44, 274–283 (2006).

7. Wu, T., Kong, X. P., Zong, X. J., Li, D. P. & Li, D. Q. Expression analysis of five maize MAP kinase genes in response to various abiotic stresses and signal molecules. Mol. Biol. Rep. 38, 3967–3975 (2011).

8. Li, H., Lin, J., Yang, Q. S., Li, X. G. & Chang, Y. H. Comprehensive analysis of differentially expressed genes under salt stress in pear (Pyrus betulaefolia) using RNA-Seq. Plant Growth Regul. 82, 409–420 (2017).

9. Sánchez-Barrena, M. J., Martínez-Ripoll, M., Zhu, J. K. & Albert, A. The structure of the Arabidopsis thaliana SOS3: Molecular mechanism of sensing calcium for salt stress response. J. Mol. Biol. 345, 1253–1264 (2005).

10. Li, S. et al. Effects of drought and salt-stresses on gene expression in Caragana korshinskii seedlings revealed by RNA-seq. BMC Genomics 17, 1–19 (2016).

11. Wang, M. et al. Comparative transcriptome analysis of salt-sensitive and salt-tolerant maize reveals potential mechanisms to enhance salt resistance. Genes and Genomics 41, 781–801 (2019).

12. Ludwig, A. A. et al. Ethylene-mediated cross-talk between calcium-dependent protein kinase and MAPK signaling controls stress responses in plants. Proc. Natl. Acad. Sci. U. S. A. 102, 10736–10741 (2005).

13. Ma, S., Gong, Q. & Bohnert, H. J. Dissecting salt stress pathways. J. Exp. Bot. 57, 1097–1107 (2006).

14. Li, K. Q., Xu, X. Y. & Huang, X. S. Identification of differentially expressed genes related to dehydration resistance in a highly drought-tolerant pear, Pyrus betulaefolia, as through RNA-Seq. PLoS One 11, 1–21 (2016).

15. Liang, Y. et al. Transcriptional regulation of bark freezing tolerance in apple (Malus domestica Borkh.). Hortic. Res. 7, 205 (2020).

16. Wu, J. et al. The genome of the pear (Pyrus bretschneideri Rehd.). Genome Res. 23, 396–408 (2013).

17. Lü, J., Tao, X., Yao, G., Zhang, S. & Zhang, H. Transcriptome analysis of low- And high-sucrose pear cultivars identifies key regulators of sucrose biosynthesis in fruits. Plant Cell Physiol. 61, 1493–1506 (2020).

18. Joo, J. H., Wang, S., Chen, J. G., Jones, A. M. & Fedoroff, N. V. Different signaling and cell death roles of heterotrimeric G protein αand β subunits in the Arabidopsis oxidative stress response to ozone. Plant Cell 17, 957–970 (2005).

19. Mittler, R. Oxidative stress, antioxidants and stress tolerance. Trends Plant Sci. 7, 405–410 (2002).

20. Suzuki, N., Koussevitzky, S., Mittler, R. & Miller, G. ROS and redox signalling in the response of plants to abiotic stress. Plant, Cell Environ. 35, 259–270 (2012).

21. Bolwell, G. P. et al. Recent advances in understanding the origin of the apoplastic oxidative burst in plant cells. Free Radic. Res. 31, (1999).

22. Huang, X. S., Wang, W., Zhang, Q. & Liu, J. H. A basic helix-loop-helix transcription factor, PtrbHLH, of Poncirus trifoliata confers cold tolerance and modulates peroxidase-mediated scavenging of Hydrogen Peroxide. Plant Physiol. 162, 1178–1194 (2013).

23. Jin, C. et al. Overexpression of a bHLH1 transcription factor of pyrus ussuriensis confers enhanced cold tolerance and increases expression of stress-responsive genes. Front. Plant Sci. 7, 1–14 (2016).

24. Yang, T. & Huang, X. S. Deep sequencing-based characterization of transcriptome of Pyrus ussuriensis in response to cold stress. Gene 661, 109–118 (2018).

25. Benjamini, Y. and Hochberg, Y. On the adaptive control of the false discovery rate in multiple testing with independent statistics. J. Educ. Behav. Stat. 25, 60–83 (2000).

26. Conesa, A., Gotz, S., Garcia-Gomez, J., Terol, J., Talon, M. and Robles, M. Blast2GO: a universal tool for annotation, visualization and ana- lysis in functional genomics research. Bioinformatics. 21, 3674–3676 (2005).

27. Langfelder, P. & Horvath, S. WGCNA: An R package for weighted correlation network analysis. BMC Bioinforma. 9, 1–13 (2008).

28. Downs, G.S., Bi, Y.M., Colasanti, J., Wu, W., Chen, X., Zhu, T., et al. A developmental transcriptional network for maize defines coexpression modules. Plant Physiol. 161, 1830–1843 (2013).

29. Pérez-Rodríguez P, Riaño-Pachón DM, Corrêa LG, Rensing SA, Kersten B, Mueller-Roeber B. PlnTFDB: updated content and new features of the plant transcription factor database. Nucleic Acids Res. 38, 822–827 (2010).

30. Chen, Q., Li, Q., Qiao, X., Yin, H. & Zhang, S. Genome-wide identification of lysin motif containing protein family genes in eight rosaceae species, and expression analysis in response to pathogenic fungus Botryosphaeria dothidea in Chinese white pear. BMC Genomics 21, 1–20 (2020).

31. Chen, C. et al. TBtools - an integrative toolkit developed for interactive analyses of big biological data. Mol. Plant. 13, 1194-1202 (2020).

32. Guo, X. et al. CNSA: A data repository for archiving omics data. Database 1–6 (2020).

33. Chen FZ, You LJ, Yang F, Wang LN, Guo XQ, Gao F, Hua C, Tan C, Fang L, Shan RQ, Zeng WJ, Wang B, Wang R, Xu X, Wei XF. CNGBdb: China National GeneBank DataBase. Yi Chuan. Aug 20;42(8):799-809 (2020).

Tables

Due to technical limitations, table 1,2 and 3 are only available as a download in the Supplemental Files section.

Figures

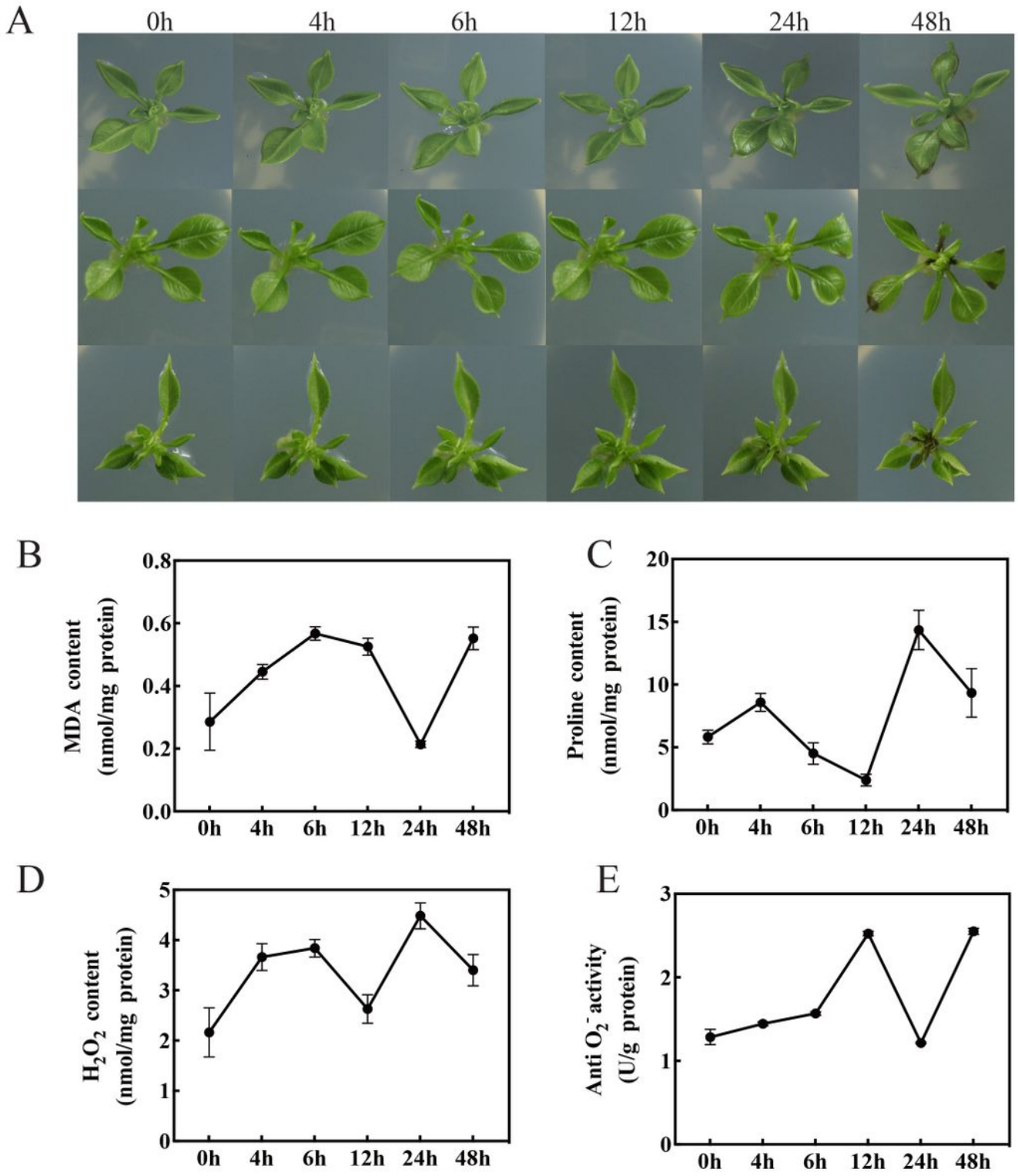

Figure 1

The phenotype and biochemical indicators of RNA-seq samples. A Phenotype of tissue cultures of pear seedling under 200 mM NaCl. B-E The relative content of four biochemical indicators. The panel shows the changes in malondialdehyde (MDA), proline (Pro), H2O2 content and anti-O2- activity at six stages and three biological replicates. Data are the mean of three biological replicates ± standard deviation.

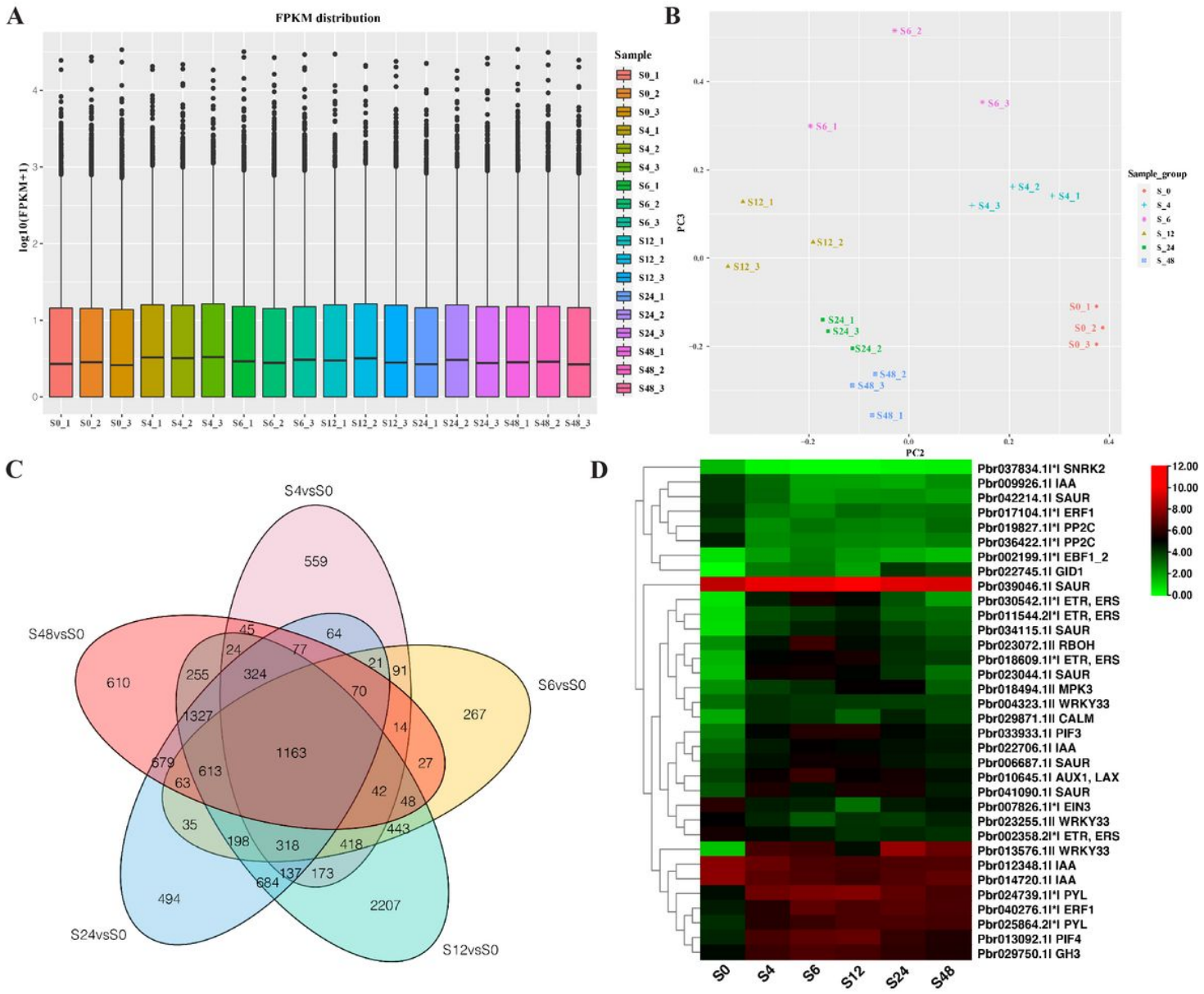

Figure 2

Comparison of pear transcriptomes at different times after starting salt treatment. A Boxplot showing the distribution of FPKM values after the imputation of missing values, fraction assignment, log10 transformation and linear regression normalization. The average of three replications for each treat timepoint sample are shown. The thick black line represents median, full line represents 1.5 times the interquartile range and dark spots represent outliers. B Principal component analysis plot showing clustering of transcriptome samples at different timepoint. Shown are the positions of each sample along with the second and third principal components (for better presentation). Colors indicate samples from different timepoint. C Number of DEGs identified by pairwise comparison of S0 vs S4, S0 vs S6, S0 vs S12, S0 vs S24 and S0 vs S4 (adjusted P<0.001 and absolute log2 fold change ≥2). D Expression profiles of plant hormone signal transduction and MAPK signal pathways related genes. Symbol '|', '||' and '|*|' indicated the genes enriched to plant hormone signal transduction pathway, MAPK signal pathway and both two pathways, respectively.

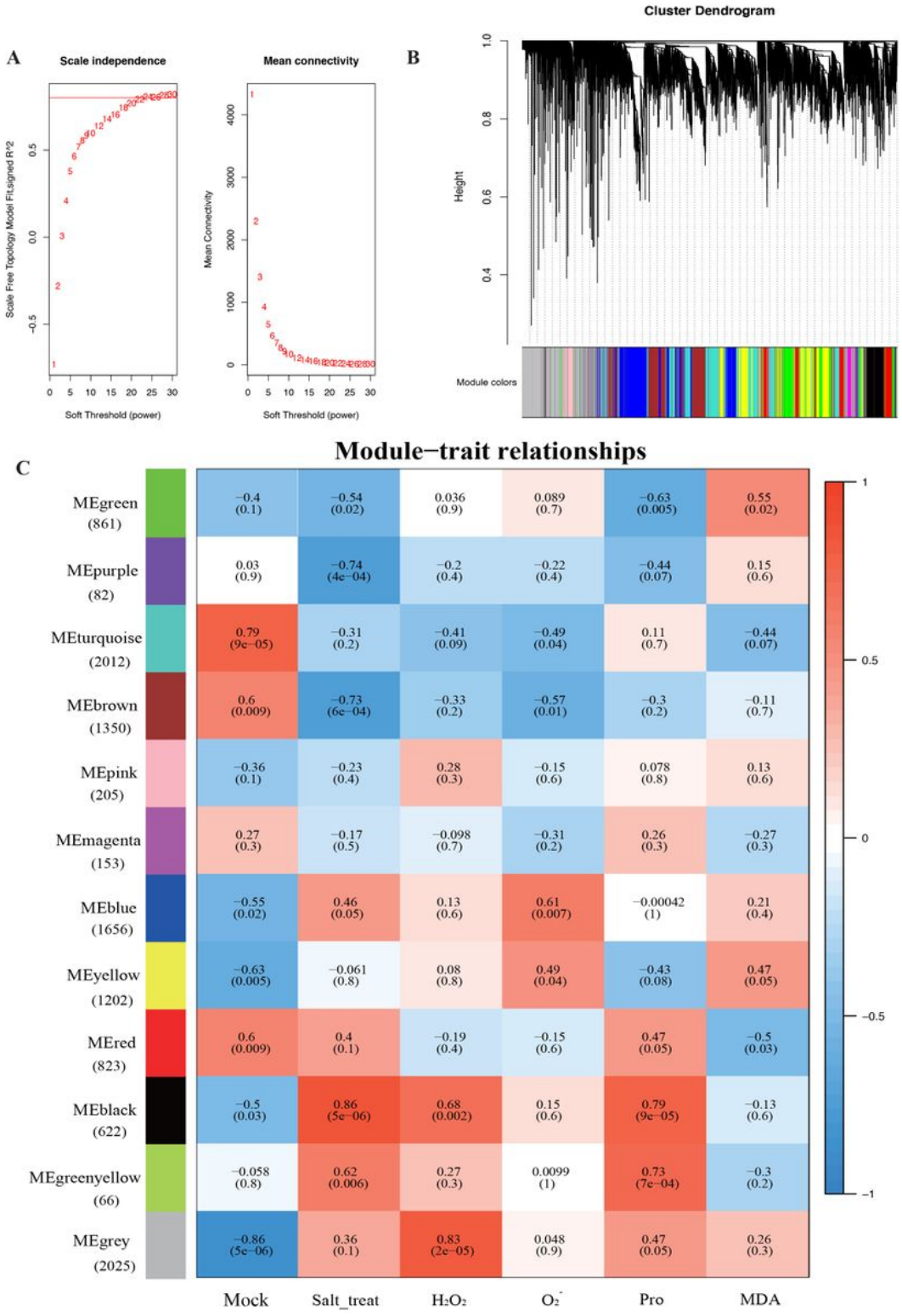

Figure 3

WGCNA of DEGs. A Network topology of different soft-thresholding powers. B Clustering dendrogram of genes with dissimilarity based on topological overlap, with assigned module colors. C Module–trait association heatmap. WGCNA grouped genes into modules based on the patterns of their co-expression. Each of the modules was labeled with a unique color as an identifier, and each row corresponds to a module. Module–trait correlations and corresponding P-values (in parentheses). The left panel shows the

12 modules, and the right panel shows the number row corresponds to a module. The number of genes in each module is indicated on the left. Each column corresponds to different traits. The color of member genes. The color scale on the middle shows module–trait correlations from-1 (blue) to 1 (red). At the bottom is the trait name. Each cell at the row–column intersection indicates the correlation coefficient between the module and trait type.

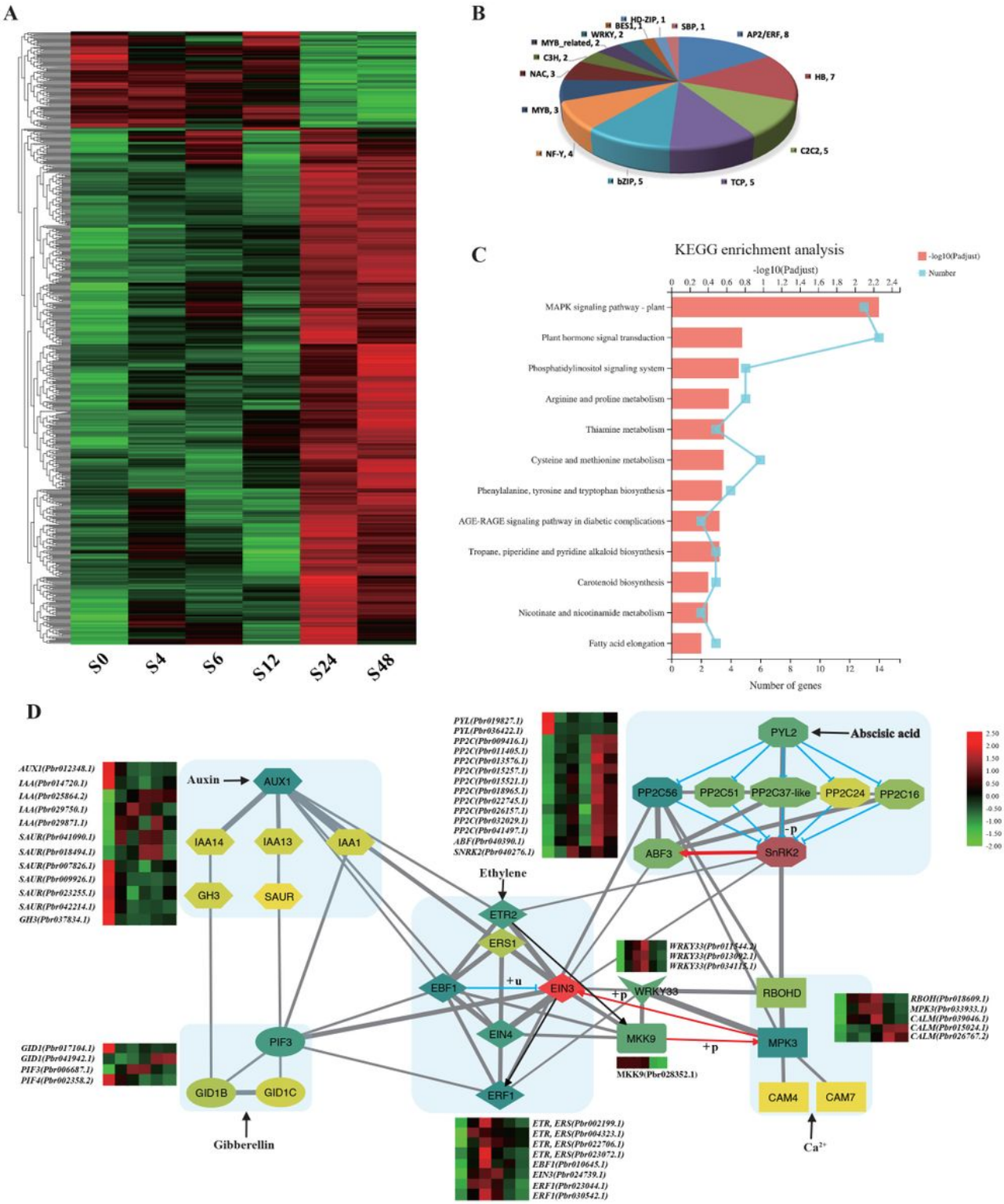

Figure 4

Expression profile and protein-protein interaction network of the black module associated with salt tolerance. A Expression profiles of genes in black module. B Distribution of the number of TFs from the black module. C KEGG enrichment of DEGs in the black module. D A consolidated protein-protein interaction network of DEGs related to plant hormone signal transduction and MAPK signal pathways displayed by Cytoscape software. Cytoscape representation of co-expressed genes with edge weights of >0.50 in the black module. Different shapes indicate the genes from each hormone related module with light blue background. The color from yellow though green to red of the node in the interactive network is proportional to the degree of the node from low to high. The width of the edge is proportional to the edge weight, and the color red and blue on the edge indicated the predicted effect of activation or inhibition to the interactive protein. Predicted effects achieved by ubiquitination, dephosphorylation and phosphorylation are indicated by symbol '+u', '-p' and '+p', respectively. The heatmaps display the expression profile of listed DEGs.

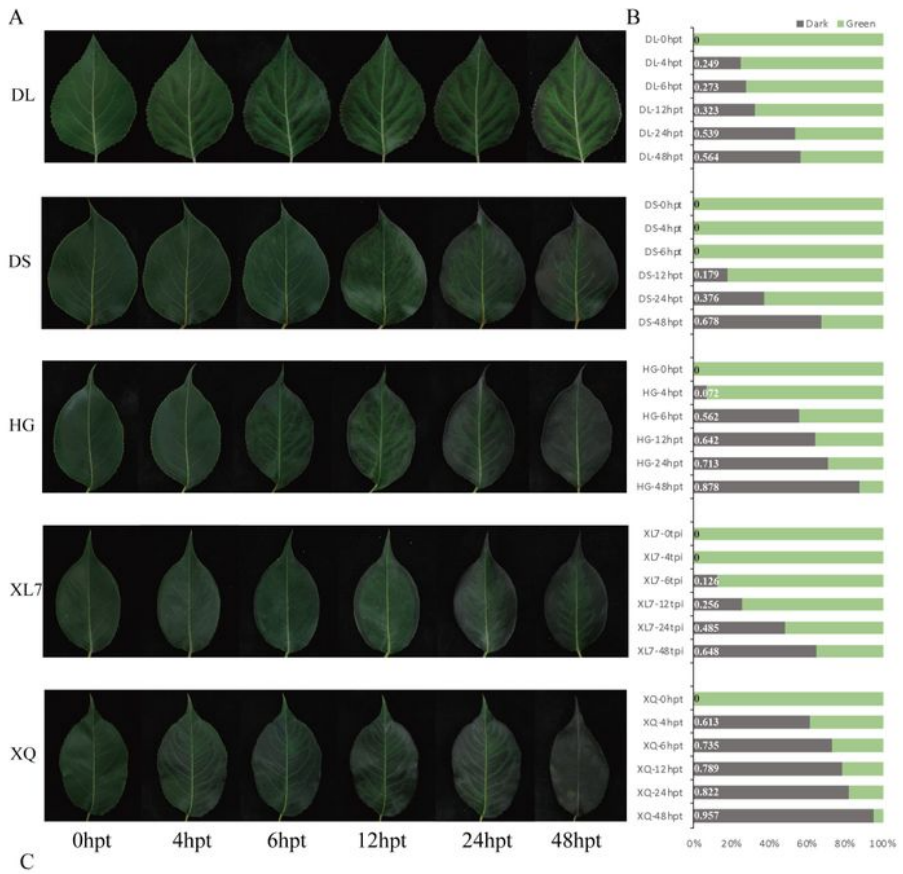

D

Gene ID	The percentage of the dark area				
	Duli	Dangshan	Huangguan	Xinli NO.7	Xueqing
IAA (Pbr025864.2)	0.884*	0.841*	-0.523	0.839*	-0.933**
ERF1 (Pbr030542.1)	0.829	0.524	0.180	0.603	-0.929**
PP2C (Pbr009416.1)	0.689	0.707	-0.928*	0.449	0.336
WRKY33 (Pbr034115.1)	0.787	0.676	0.712	0.832*	0.634
SAUR1 (Pbr041090.1)	-0.110	0.627	-0.913*	0.730	0.539
ETR/ERS (Pbr023072.1)	-0.418	0.492	-0.757	-0.121	-0.496

Figure 5

Connection of predicted genes and salt tolerance. A The phenotype of five varieties under salt treatment. B The dark/green ratios of the treated leaves from different pear cultivars. C Relative expression level of six selected genes in different pear cultivars under salt treatment. D Linear regression coefficient between gene expression and salt tolerance. Results are presented as means of three biological replicates ± standard deviation, and significant differences are marked with *P<0.05 or **P< 0.01.

Supplementary Files

This is a list of supplementary files associated with this preprint. Click to download.

- Table1.xlsx
- Table2.xlsx
- Table3.xlsx
- Additionalfile1.pdf
- Additionalfile2.pdf
- Additionalfile3.pdf
- Additionalfile4.xlsx